

# Effects of Airstream Mach Number on H<sub>2</sub>/N<sub>2</sub> Plasma Igniter

Goro Masuya,\* Kenichi Takita,† Katsuyoshi Takahashi,‡ Fumio Takatori,‡ and Hiroyuki Ohzeki§  
Tohoku University, Miyagi 980-8579, Japan

**Experimental study of the plasma igniter was conducted in nonheated high-speed air stream. The effects of the Mach number, from 0.9 to 2.4, and the stagnation pressure of the airstream, from 64 to 100 kPa, as well as the hydrogen fraction in the H<sub>2</sub>/N<sub>2</sub> feedstock of the torch, from 0 to 50%, were investigated. In the higher Mach number airstream, more input power to the torch was required to ignite hydrogen fuel. The stagnation pressure of the airstream had complicated effects relating to chemistry and aerodynamics. Improvement of ignition performance due to the increased hydrogen fraction in the feedstock was well correlated with the sum of the electric input energy and the heat of combustion of the hydrogen fed as the feedstock of the torch.**

## Nomenclature

$d$	= diameter
$h$	= specific enthalpy
$I$	= peak intensity in emission spectrum
$M$	= Mach number
$m$	= mass flow rate
$P$	= power of plasma torch
$p$	= pressure
$q_c$	= heat of combustion per unit mass of fuel
$x, y, z$	= Cartesian coordinates
$\chi$	= mole fraction

## Subscripts

$a$	= air
$av$	= average
$HF$	= hydrogen fuel
$HPJ$	= hydrogen in feedstock
$i$	= injector
$IN$	= input
$PJ$	= plasma torch
$PJ + F$	= plasma torch and fuel injection
$t$	= stagnation condition
$total$	= sum of electric and combustion energies
$0$	= undisturbed freestream

## Introduction

ONE of the most important technologies for dual-mode scramjet engines is reliable ignition of the fuel. The dual-mode scramjet is required to operate from a flight Mach number of 4 or lower. In the low Mach number range, temperature of the airstream is not high enough to achieve autoignition of hydrogen,<sup>1</sup> and igniters should be installed in the engine. Various kinds of igniters have

been tested for scramjet combustors.<sup>2,3</sup> The plasma torch is one of the promising igniters. Plasma torches have been tested not only in direct-connect combustors<sup>4–6</sup> but also in a subscale engine.<sup>7</sup> Ignition mechanism of hydrogen by the plasma torch has been investigated both in analytical<sup>8,9</sup> and numerical<sup>10</sup> approaches.

In the subscale engine test at the simulated flight condition of Mach 4 and 20 km altitude, the plasma torch could successfully ignite both the pilot fuel and the main fuel.<sup>7</sup> However, at a Mach 6 condition, the torch failed to ignite the main fuel in the same engine with a low contraction ratio configuration such as the one used in the Mach 4 test.<sup>7</sup> A strut was installed in the engine to increase the contraction ratio of the air intake, and it resulted in successful ignition of the fuel.<sup>11</sup> The strut lowered the combustor Mach number and lead to higher static pressure and temperature, as well as to reduced velocity, all of which were favorable to ignition. However, the effect of the Mach number on the ignition performance of the plasma torch has not been tested at well-defined conditions to identify these various effects.

Another important factor for the ignition performance of the plasma igniter is the choice of the feedstock. Adding small amount of hydrogen to the feedstock of argon significantly improved the performance of the plasma igniter.<sup>6</sup> If this improvement was brought about by the H radical produced in the plasma jet, a similar favorable effect may occur by adding hydrogen to other feedstock, such as oxygen or nitrogen. The H<sub>2</sub>/N<sub>2</sub> mixture is more desirable from the safety viewpoint.

The purpose of the present study is to investigate experimentally the effects of the airstream Mach number and hydrogen fraction in the H<sub>2</sub>/N<sub>2</sub> feedstock on the ignition characteristics of the plasma torch igniter.

## Experimental Apparatus

### Wind Tunnel

The experiment was conducted using a suction-type wind tunnel, shown in Fig. 1, with a vacuum tank of 8 m<sup>3</sup>. When a gate valve between the test section and the evacuated tank was opened, atmospheric air was inhaled through a supersonic nozzle. Figure 2 shows details of the nozzle and the test section. Three nozzles with different designed Mach numbers were used in the present study. Their walls were two dimensionally contoured. All of the nozzles had the same square exit section of 30 × 30 mm.

When the effect of the stagnation pressure of the undisturbed airstream was investigated, a duct with a perforated plate and/or screens was attached upstream of the nozzle. Four screens were placed at a distance of 4.5 mm. The perforated plate had several circular holes, with different diameters, and total area of the holes was 0.49 of the cross-sectional area of the duct. The screens reduced the freestream stagnation pressure  $p_{t0}$  from 100 to 76 kPa and the addition of the perforated plate reduced it to 64 kPa. The test section was 310 mm long, and it had a constant square cross section, which

Presented as Paper 2001-0520 at the AIAA 39th Aerospace Sciences Meeting and Exhibit, Reno, NV, 8–11 January 2001; received 25 April 2001; revision received 6 November 2001; accepted for publication 10 December 2001. Copyright © 2002 by the American Institute of Aeronautics and Astronautics, Inc. All rights reserved. Copies of this paper may be made for personal or internal use, on condition that the copier pay the \$10.00 per-copy fee to the Copyright Clearance Center, Inc., 222 Rosewood Drive, Danvers, MA 01923; include the code 0748-4658/02 \$10.00 in correspondence with the CCC.

\*Professor, Department of Aeronautics and Space Engineering, Aoba-yama 01, Sendai. Senior Member AIAA.

†Assistant Professor, Department of Aeronautics and Space Engineering, Aoba-yama 01, Sendai. Member AIAA.

‡Graduate Student, Department of Aeronautics and Space Engineering, Aoba-yama 01, Sendai.

§Student, Department of Aeronautics and Space Engineering, Aoba-yama 01, Sendai.

was the same as the nozzle exit. The sidewalls of the test section were made of quartz glass.

The freestream Mach number  $M_0$  for each nozzle was deduced from the wall pressure in the middle region of the test section, where the plasma torch was placed, with an isentropic relation, and the deduced value of  $M_0$  was 0.9, 1.8, and 2.4 for the designed value of 1.5, 2.0, and 2.5, respectively. The Mach number at the inlet of the test section was slightly further away from unity than  $M_0$ , typically 0.05. For the nozzle of the designed Mach number 1.5, the wall friction in the test section caused choking at the exit of the test section. A shock wave system might be produced in the nozzle, and the estimated  $M_0$  of 0.9 might be too high.

The airstream conditions tested were summarized in Table 1. Note that the values in the lowest column were evaluated assuming  $M_0 = 0.9$  and  $p_{t0} = 100$  kPa. The subscale engine tests are usually conducted at the stagnation conditions of the real flight, for example,  $p_{t0} = 860$  kPa and  $T_{t0} = 870$  K for Mach 4 flight at 20-km altitude.<sup>7</sup> The inlet Mach number of the combustor may be one-half or one-third of the flight Mach number. Therefore, the temperature and pressure at the combustor inlet of the subscale engine are higher

than those of the present experiment. This means that, for ignition of hydrogen, the present airstream conditions were much less favorable than those observed in the combustor of the subscale engine tests. In addition, there was no backward-facing step in the present test section where low-speed flow could be trapped. If the plasma torch could ignite the fuel in these conditions, it would also be possible to ignite the fuel in the subscale engine.

Plasma Torch

Configuration

The plasma torch was attached on the bottom wall of the test section, as shown in Fig. 2. The torch configuration shown in Fig. 3 was basically same as that installed in the subscale scramjet engine<sup>7</sup> except for the change in the coolant from gas to water to allow higher input electric power. This type of torch configuration was employed because its ignition performance and operational characteristics have been intensively studied in the direct connect tests of supersonic combustors<sup>6,8,12–15</sup> as well as in subscale engine tests.<sup>7,11</sup> The present study will add further information on the characteristics of the plasma torch igniter and improve its ignition performance.

The cathode was made of hafnium to attain high durability when oxygen or air was used as feedstock. The anode and nozzle were made of oxygen-free copper. The diameter of the torch nozzle throat,  $d$ , was 1.5 mm. The origin of the Cartesian coordinate system ( $x, y, z$ ) was taken at the center of the torch nozzle exit. The feedstock of the torch was either pure nitrogen or a hydrogen/nitrogen

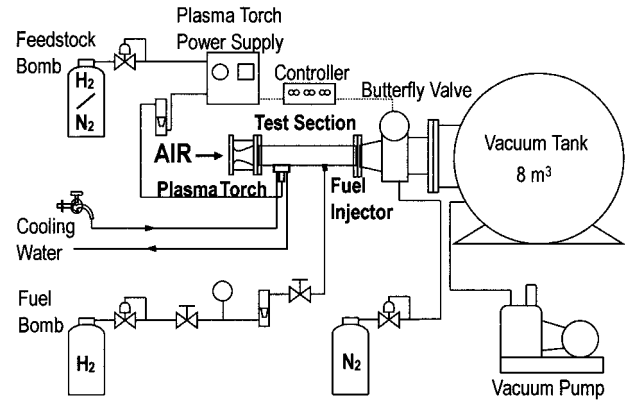


Fig. 1 Schematic diagram of experimental apparatus.

Table 1 Freestream conditions

$M_0$	$p_{t0}$ , kPa	$T_{t0}$ , K	$p_0$ , kPa	$T_0$ , K	$m_a$ , g/s	$m_a h_{ta}$ , kW	$Re$ , 1/m
2.4	100	280	6.8	130	74	20.7	$4.0 \times 10^5$
1.8	100	↑	17.4	179	126	35.3	$5.0 \times 10^5$
↑	76	↑	13.2	↑	93	26.0	$3.8 \times 10^5$
↑	64	↑	11.1	↑	79	22.1	$3.2 \times 10^5$
0.9	100	↑	59.1	241	183	51.3	$5.6 \times 10^5$

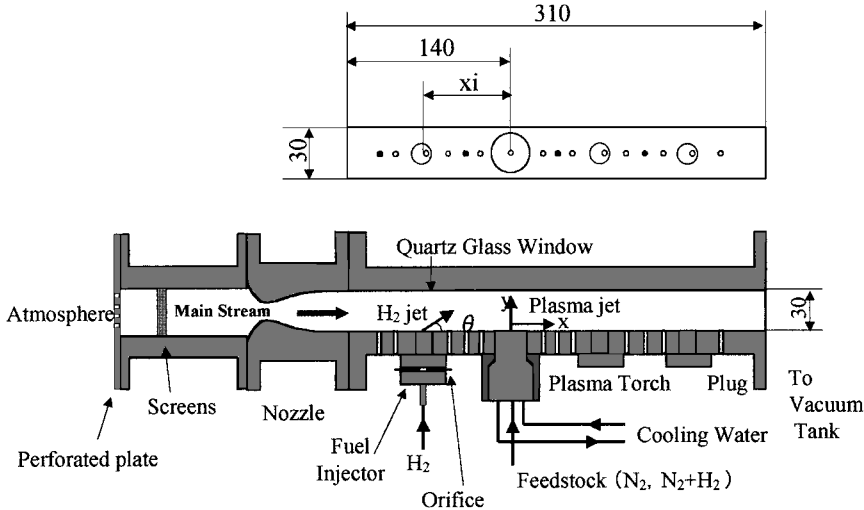


Fig. 2 Nozzle and test section (dimensions in millimeters).

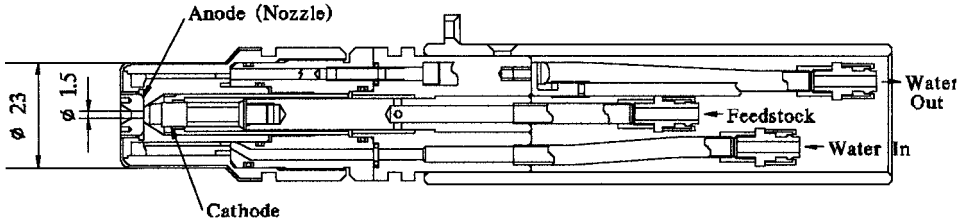


Fig. 3 Plasma torch (dimensions in millimeters).

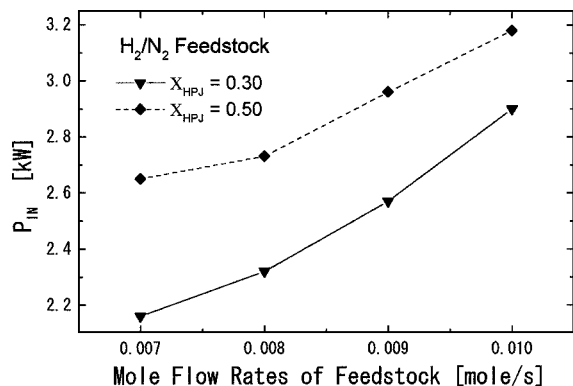


Fig. 4 Lowest input power of  $H_2/N_2$  plasma torch:  $\blacktriangle$ ,  $X_{HPJ} = 0.30$ ; and  $\blacklozenge$ ,  $X_{HPJ} = 0.50$ .

mixture. The hydrogen mole fraction of the mixed gas,  $X_{HPJ}$ , was 0.02, 0.10, 0.30, or 0.50. The molar flow rate of the nitrogen feedstock was  $1.1 \times 10^{-2}$  mol/s unless another value is specified in the paper. The molar flow rates of the  $H_2/N_2$  mixtures were inversely proportional to the square root of the mean molecular mass of the mixtures and were  $1.1 \times 10^{-2}$  mol/s and  $1.5 \times 10^{-2}$  mol/s for  $X_{HPJ} = 0.02$  and 0.50, respectively. The dc power unit supplied 1.5–5.5 kW of electric power,  $P_{IN}$ , to the torch.

#### Lowest Required Power of $H_2/N_2$ Torch

As hydrogen fraction in the feedstock increased, higher input electric power was required to start and maintain stable operation of the plasma torch because of the high ionization energy of hydrogen. In Fig. 4, the lowest input power for stable operation of the torch was plotted to the mole flow rate of the feedstock. For  $X_{HPJ} \leq 0.10$ , the torch could operate at the lowest possible power of the power supply equipment, namely, about 1.5 kW. For  $X_{HPJ} \geq 0.30$ , the lowest input power increased with  $X_{HPJ}$  and flow rate of the feedstock.

#### Exhaust from Plasma Torch

The color of the plasma jet ejected into the quiescent atmosphere turned from violet–blue of pure nitrogen to purple–red by adding hydrogen. While electric power was supplied to the plasma jet, it was not possible to observe directly weak emission from hydrogen flame because of strong emission from the plasma torch. However, if the supply of the feedstock with a high hydrogen fraction was not stopped after the electric current to the plasma torch was turned off, the flame was seen at the exit of the torch nozzle. It is quite reasonable that the hot hydrogen in the plasma jet burned with the surrounding air, too.

#### Fuel Injector

The fuel was gaseous hydrogen at the room temperature and was injected at sonic speed from one of circular orifices of 1.5 mm diam on the sone line of the bottom wall as shown in Fig. 2. The injector location was represented by the center of the injector block and denoted by  $x_i$ . However, actual position of the injection hole was 2 mm downstream of the nominal value of  $x_i$ . The reference mass flow rate of the fuel was 0.10 g/s for  $M_0 = 1.8$  and  $p_{t0} = 100$  kPa. This fuel mass flow rate and the mass flow rate of the airstream shown in Table 1 resulted in the fuel equivalence ratio of 0.027. The fuel injection angle  $\theta$  was fixed to 90 deg because the effect of  $\theta$  was not significant for the present injection condition.<sup>12</sup>

#### Instrumentation

The wall pressure distribution was measured using a mechanical pressure scanner with a strain-gauge-type sensor. The signal from the sensor was amplified by a dc amplifier, digitized by a 12-bit A/D converter, and recorded on a personal computer. The accuracy of the pressure measurement system is estimated as  $\pm 1\%$ .

The spectral intensity of emission of the plasma jet was measured by a spectrometer (Ritsu MC-8). The wavelength range of the

spectrometer was 250–950 nm, and the incident slit width and the line density of diffraction grating were 0.5 mm and 300 lines/mm, respectively. No correction was made for the decay of the spectral signal in the glass fibers. However, it had little influence on the present study because we concentrated on the peak of the H atom at 656 nm and that of the N atom at 410 nm for which the decay in the glass fiber was not significant. Absorption of the emission by the quartz glass used for the windows of the test section was confirmed as negligibly small. Emission from a source in the test section was received by an optical probe located at  $(x, y, z) = (0, 4, 30)$  mm and transmitted to the spectrometer by glass fibers. The spectral intensity was proportional to the sampling time unless the sensor was saturated. In the present experiment, the exposure time was either 85 or 100 ms, and the results for sampling time of 85 ms were adjusted to those of 100 ms. This exposure time was long, and only the steady feature of the emission was measured in the present experiment.

The flow rates of the fuel and feedstock were measured by float-type flow meters. The flow rate of the airstream was calculated assuming that the discharge coefficient of the nozzle throat was unity.

The schlieren and direct photographs were taken through the windows of the side walls. A stroboscopic light of 70-ns pulse time or a continuous mercury lamp was used to take the schlieren photograph.

## Results and Discussion

### Effect of Mach Number on Ignition Limit

Figure 5 shows axial distributions of the wall pressure nondimensionalized by the freestream stagnation pressure  $p/p_{t0}$  for three values of the freestream Mach number. The feedstock of the torch was nitrogen, and the axial location of the fuel injector,  $x_i$ , was 40d upstream of the torch ( $x_i/d = -40$ ). Flow rates of the fuel and the feedstock were kept constant. Operation of the plasma torch resulted in a slight pressure rise downstream of the torch nozzle. In the Mach 1.8 and 2.4 flows, fuel injection caused only a small change for the lowest torch input power, namely,  $P_{IN} = 1.5$  kW. However, further increase of  $P_{IN}$  resulted in a significant pressure rise in the downstream region. In the Mach 0.9 flow, on the other hand, pressure decreased by fuel injection for all nonzero value of  $P_{IN}$ . Relations between  $P_{IN}$  and the pressure at  $x/d = 60$  are summarized in Fig. 6. The pressure is nondimensionalized by the undisturbed wall pressure  $p_0$  at  $x/d = 60$ . Significant departure between the pressures with and without fuel injection occurred at  $P_{IN} \geq 1.7$  and 2.1 kW for  $M_0 = 1.8$  and 2.4, respectively. Result for lower fuel flow rate to match the fuel–air ratio of  $M_0 = 2.4$  with that of  $M_0 = 1.8$  is also shown in Fig. 6. There was no difference between the ignition limits of these two fuel flow rates. For  $M_0 = 0.9$ , the pressure decrease due to the heat addition by combustion of fuel was observed even at  $P_{IN} = 1.5$  kW, which was the lowest value achievable by the power supply unit for the torch. Therefore, the ignition limit in  $P_{IN}$  for  $M_0 = 0.9$  was lower than 1.5 kW. These results clearly showed that the ignition limit in  $P_{IN}$  increased with  $M_0$  for the same stagnation conditions.

### Effect of Pressure on Ignition Limit

Changing Mach number at the constant stagnation condition also results in changes of static pressure and temperature. To separate the effect of the static pressure from that of the Mach number, an experiment with reduced  $p_{t0}$  was carried out using the perforated plate and/or the screens. As shown in Table 1,  $p_{t0}$  was reduced as low as two-thirds of the atmospheric pressure. There were no observed significant changes in schlieren photographs and nondimensional pressure distributions of the undisturbed flow at reduced  $p_{t0}$ .

Figure 7 shows the influence of the stagnation pressure on the ignition limit of  $P_{IN}$ . In Fig. 7, the abscissa was the input power per unit mass of the airstream,  $P_{IN}/m_a$ , because this quantity governs the temperature and pressure rises downstream. The calculation of the finite-rate reaction<sup>9</sup> in the pressure range from 10 to 20 kPa predicted that the ignition delay time of the hydrogen–air mixture with a small amount of radicals would increase with decrease of the pressure. The same calculation predicted an opposite tendency

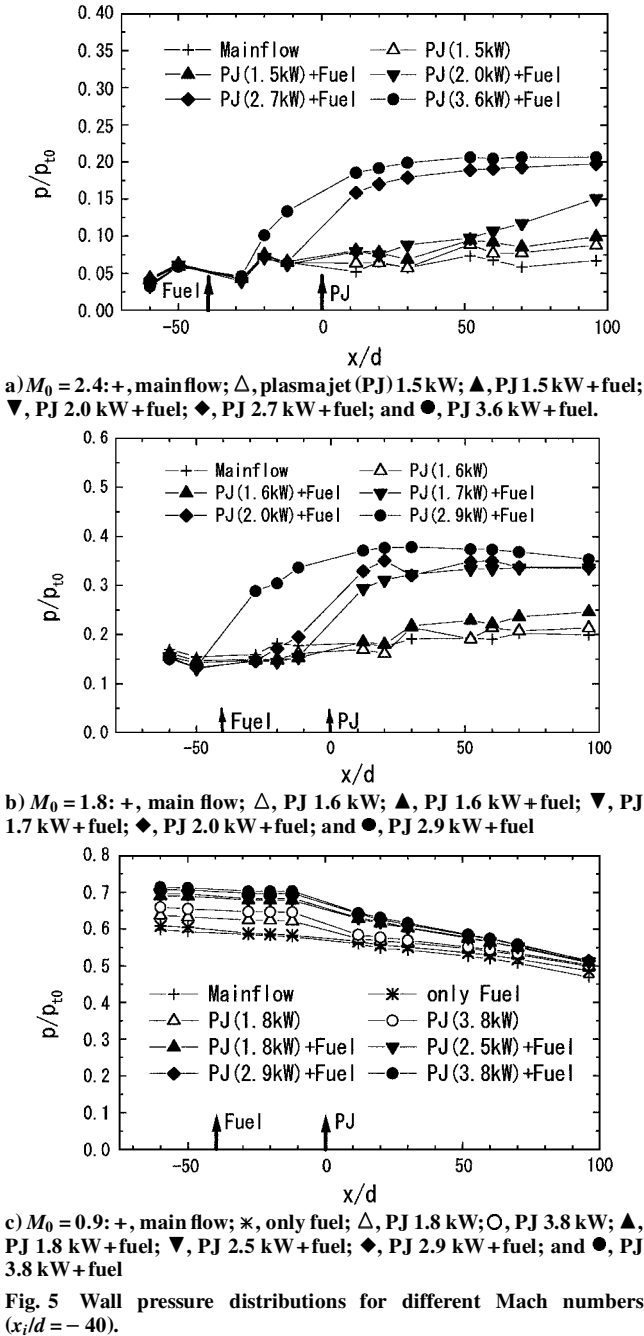


Fig. 5 Wall pressure distributions for different Mach numbers ( $x_i/d = -40$ ).

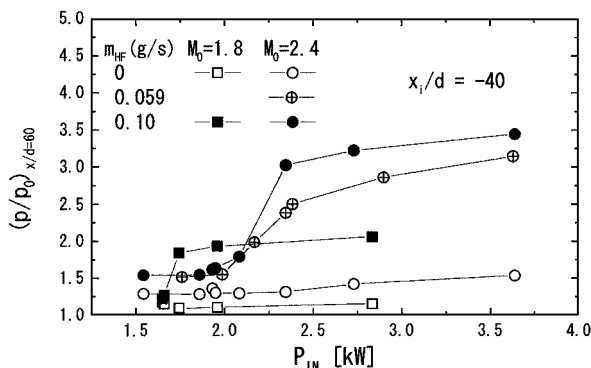


Fig. 6 Effect of Mach number on ignition performance:  $\square$ ,  $M_0 = 1.8$  and  $m_{HF} = 0$  g/s;  $\blacksquare$ ,  $M_0 = 1.8$  and  $m_{HF} = 0.10$  g/s;  $\circ$ ,  $M_0 = 2.4$  and  $m_{HF} = 0$  g/s;  $\oplus$ ,  $M_0 = 2.4$  and  $m_{HF} = 0.059$  g/s; and  $\bullet$ ,  $M_0 = 2.4$  and  $m_{HF} = 0.10$  g/s.

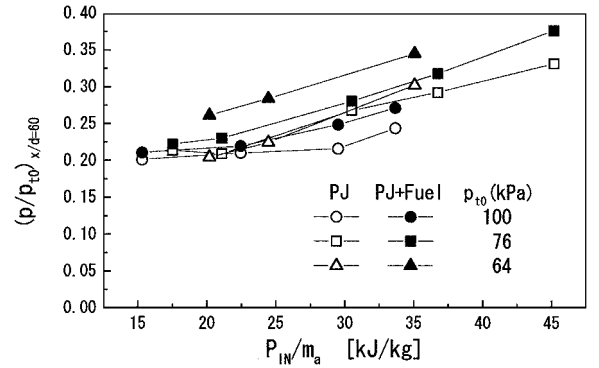


Fig. 7 Effect of pressure on ignition performance: open symbols, PJ and solid symbols, PJ + fuel;  $\circ$ ,  $p_0 = 100$  kPa;  $\square$ ,  $p_0 = 76$  kPa; and  $\Delta$ ,  $p_0 = 64$  kPa.

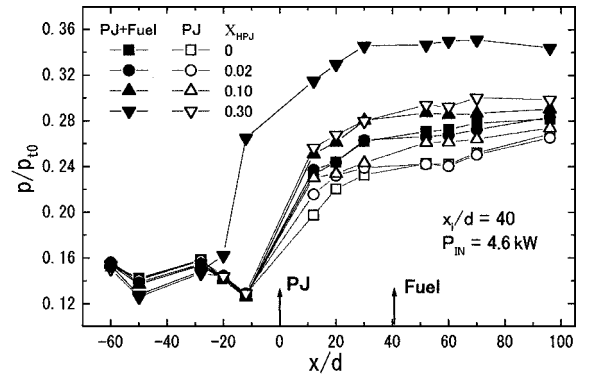


Fig. 8 Effect of  $H_2$  fraction of feedstock on wall pressure distributions,  $M_0 = 1.8$ , and  $P_{IN} = 4.6$  kW: open symbols, PJ and solid symbols, PJ + fuel;  $\square$ ,  $X_{HPJ} = 0$ ;  $\circ$ ,  $X_{HPJ} = 0.02$ ;  $\Delta$ ,  $X_{HPJ} = 0.10$ ; and  $\nabla$ ,  $X_{HPJ} = 0.30$ .

for the pressure, more than about 60 kPa. The latter tendency was caused by the increased three-body reaction producing  $HO_2$ . Such a tendency in the autoignition in the  $H_2$ -air supersonic combustor was discussed by Sung et al.<sup>16</sup> However, the comparison between this prediction and the present experimental results was not straightforward. When  $p_0$  was 64 kPa, fuel injection caused a significant pressure rise for the whole range of  $P_{IN}/m_a$  tested in the present experiment. However, the pressure difference between the cases with and without fuel injection for  $P_{IN}/m_a \approx 30$  kJ/kg was negligible for  $p_0 = 76$  kPa, whereas it was significant for  $p_0 = 100$  kPa. At  $P_{IN}/m_a \approx 30$  kJ/kg, ignition occurred for  $p_0 = 64$  and 100 kPa, but did not for  $p_0 = 76$  kPa. The relation between the data for  $p_0 = 100$  and 76 kPa qualitatively agreed with the theoretical prediction,<sup>9</sup> but that for  $p_0 = 76$  and 64 kPa contradicted the prediction. The latter relation might be governed by the aerodynamic phenomenon rather than the chemical reaction. The wall boundary layers observed in the schlieren photograph became thicker for lower  $p_0$  and, thus, lower Reynolds number. The wall pressure distribution of the lower  $p_0$  resulted in a higher rate of pressure rise due to the effect of wall friction. The thick boundary layer was easier to separate than the thin boundary layer. Once separation occurred, it would provide a more favorable condition to ignite the fuel for the same value of  $P_{IN}/m_a$  at the same Mach number.

### Effect of Hydrogen Fraction in Feedstock

#### Effect of $H_2/N_2$ Torch on Flow Without Fuel Injection

The pressure distributions with the plasma torch operating at  $P_{IN} = 4.6$  kW for various values of  $X_{HPJ}$  are shown in Fig. 8. Open symbols and solid symbols are data with and without fuel injection, respectively.

When  $P_{IN}$  was kept constant without fuel injection, pressure downstream of the plasma torch increased with  $X_{HPJ}$ . The distribution for  $X_{HPJ} = 0.50$ , not shown in Fig. 8, was very high throughout

the test section, showing that the thermal choking occurred in the test section. This result indicated that more heat was added to the airstream as the hydrogen fraction of feedstock became higher. We examined two possible reasons for this phenomenon: One was increase of the ratio of thermal output to the electric input, namely, thermal efficiency of the plasma torch, and the other was the combustion of hydrogen in the feedstock with air.

Sakuranaka et al.<sup>14</sup> measured the thermal efficiency of a water-cooled plasma torch with various kinds of feedstock including oxygen, nitrogen, and argon/hydrogen. The efficiency for  $N_2$  or  $O_2$  was about 0.8, whereas that for  $H_2/Ar$  increased from 0.5 for pure argon to 0.7 as the hydrogen fraction increased. Barbi et al.<sup>17</sup> reported higher thermal efficiency for an  $H_2/Ar$  uncooled plasma torch, and the efficiency increased from 0.84 to 0.92 with the hydrogen fraction of the feedstock. These results suggest that the thermal efficiency of the  $H_2/N_2$  and  $H_2/Ar$  torches would not change much with the hydrogen fraction. Therefore, the improvement of the thermal efficiency of the torch with increase of  $X_{HPJ}$  was not likely the reason for the wall pressure rise shown in Fig. 8.

If we approximate the flow as the Rayleigh flow of air with Mach 1.7, which was estimated at the exit of the test section where the choking might occur, the heat required to thermally choke the flow was about 16% of the stagnation enthalpy of the airstream. The sum of the thermal output of the torch and the heat of combustion of the hydrogen in the feedstock of  $X_{HPJ} = 0.50$  was estimated to be about 21% of the stagnation enthalpy of the airstream. This estimated value of the heat addition was above the value required for thermal choking. Thus, the hydrogen in the feedstock burned in the low-pressure, low-temperature, supersonic airstream, as well as in the quiescent atmospheric air, and resulted in the pressure rise.

#### Ignition Limit

The open symbol data in Fig. 8 show the effect of  $X_{HPJ}$  on the wall pressure distribution when fuel was injected 60 mm downstream of the torch nozzle ( $x_i/d = 40$ ). Because  $P_{IN}$  for the data shown were rather high, all of the fuel-injection data (open symbols) downstream of the torch were higher than the corresponding noninjection data (solid symbols). These distributions indicate that the fuel was ignited in these cases.

Figure 9 shows the effect of the input power on the average wall pressure downstream of the torch for fuel injection at  $x_i/d = 30$ . The average of the pressures measured at all of the taps downstream of the torch was used for comparison to avoid the fluctuation of data due to nonmonotonous change of pressure in the  $x$  direction caused by waves in the supersonic stream. When pure nitrogen was used as the feedstock, there was almost no difference observed between noninjection data (open squares) and injection data (solid squares) for  $P_{IN} < 2.8$  kW. The averaged pressure with fuel injection became higher than that without fuel injection at  $P_{IN} = 3.5$  kW and higher. The pressure rise due to ignition was observed at  $P_{IN} = 2.9$  kW by adding 2% of hydrogen to the feedstock. When  $X_{HPJ} = 0.30$ , the pressure rise was seen at  $P_{IN} = 2.6$  kW, which was the lower limit of

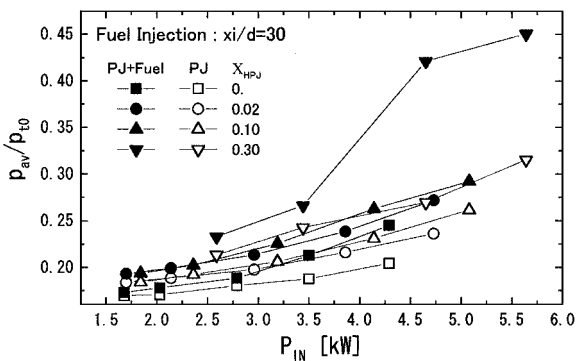


Fig. 9 Effect of  $H_2$  fraction of feedstock on average wall pressure downstream of plasma torch nozzle: open symbols, PJ and solid symbols, PJ + fuel;  $\square$ ,  $X_{HPJ} = 0$ ;  $\circ$ ,  $X_{HPJ} = 0.02$ ;  $\triangle$ ,  $X_{HPJ} = 0.10$ ; and  $\nabla$ ,  $X_{HPJ} = 0.30$ .

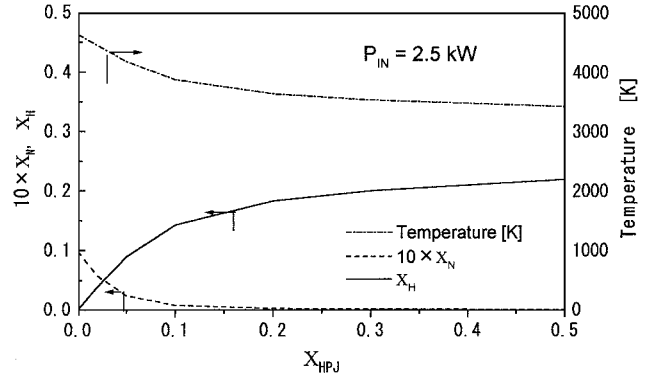


Fig. 10 Calculated properties of chemically equilibrium plasma jet at the nozzle throat: —,  $X_H$ ; ---,  $10 \times X_N$ ; and ---,  $T$ .

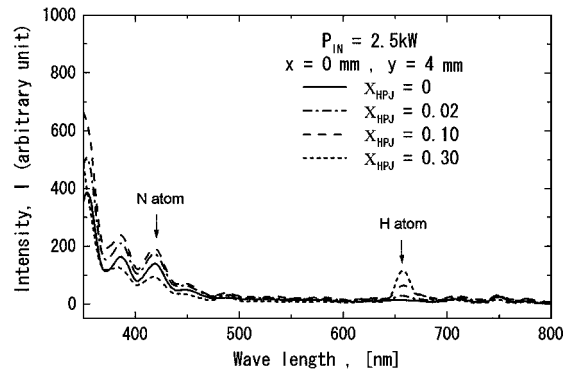


Fig. 11 Spectra of emission from  $H_2/N_2$  plasma jets: —,  $X_{HPJ} = 0$ ; ---,  $X_{HPJ} = 0.02$ ; ----,  $X_{HPJ} = 0.10$ ; and ···,  $X_{HPJ} = 0.30$ .

$P_{IN}$  for the stable operation of the torch for this  $H_2$  fraction. Further pressure rises for  $P_{IN} > 4.5$  kW with  $X_{HPJ} = 0.30$  were caused by thermal choke.

#### Estimation of Radical Fraction

One of the possible mechanisms to enhance ignition performance by adding hydrogen to the feedstock is the increase of radicals in the plasma jet. Qualitative estimation of the radical fraction was made by use of theoretical and experimental approaches.

Theoretical calculation of the compositions of the plasma jets was made by assuming that the plasma jet was a uniform flow in thermochemical equilibrium. The thermal conversion rate of the input electric energy was set as 80%, based on the measurement of the water-cooled torch by Sakuranaka et al.<sup>14</sup> Figure 10 shows calculated temperature and mole fractions of H and N atoms at the throat of the torch nozzle for  $P_{IN} = 2.5$  kW. The temperature of the plasma jet was moderately reduced by addition of hydrogen to the feedstock while the fractions of the radicals were changed more significantly. The N atoms were quickly annihilated, but the H atoms were produced much more than the N atoms reduced.

Experimental estimation of the radical fraction was made by comparing the peak intensities in the spectra of emission from the plasma jets measured at  $x = 0$  mm and  $y = 4$  mm in the Mach 1.8 airstream. Typical spectra are shown in Fig. 11 for various values of  $X_{HPJ}$ . Intensities of the peaks corresponding to the N atom at the wavelength of 410 nm and the H atom at 656 nm are normalized by the corresponding intensities for  $X_{HPJ} = 0.02$  and  $P_{IN} = 2.5$  kW and are shown in Fig. 12. Note that these intensities are only qualitative indexes of the radical fraction. The intensity of the H atom monotonously increased with  $X_{HPJ}$  and  $P_{IN}$ . The emission intensity of the N atom at 410 nm first increased and then decreased with increase of  $X_{HPJ}$ . This change is quite different from that expected from the equilibrium calculation and suggests that the assumption of uniform flow in chemical equilibrium may not be applicable to the present plasma jets.

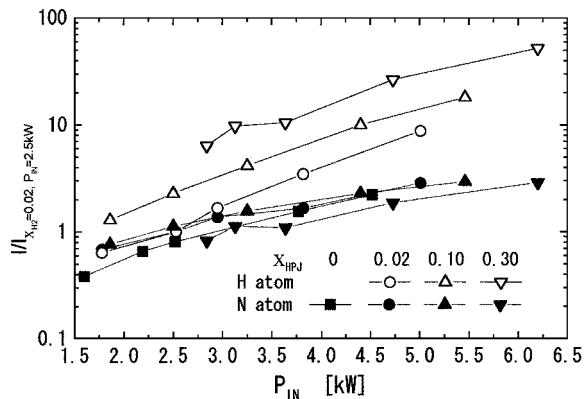


Fig. 12 Relative change of spectral intensity of radicals in  $H_2/N_2$  plasma jet:  $x = 0$  mm and  $y = 4$  mm; open symbols, H atom; solid symbols, N atom;  $\square$ ,  $X_{HPJ} = 0$ ;  $\circ$ ,  $X_{HPJ} = 0.02$ ;  $\triangle$ ,  $X_{HPJ} = 0.10$ ; and  $\nabla$ ,  $X_{HPJ} = 0.30$ .

The finite-rate chemical calculation<sup>9</sup> of the ignition in the  $H_2$ -air mixture predicted that the O radical was more effective for ignition enhancement than the H radical when the same moles were added to the mixture. The N atom was as effective as the O atom because the N atom immediately reacted with the  $O_2$  molecule in the air to produce the O atom. However, the effectiveness of the O atom and the N atom was only several times of that of the H atom. The mole fraction of the H atom estimated by the chemical equilibrium calculation shown in Fig. 10 was much larger than that of the N atom for the pure nitrogen feedstock. Therefore, remarkable improvement of the ignition performance of the torch was expected by adding hydrogen to the feedstock of nitrogen. However, the result of the ignition test showed only a rather gradual improvement by increasing the hydrogen fraction in the feedstock.

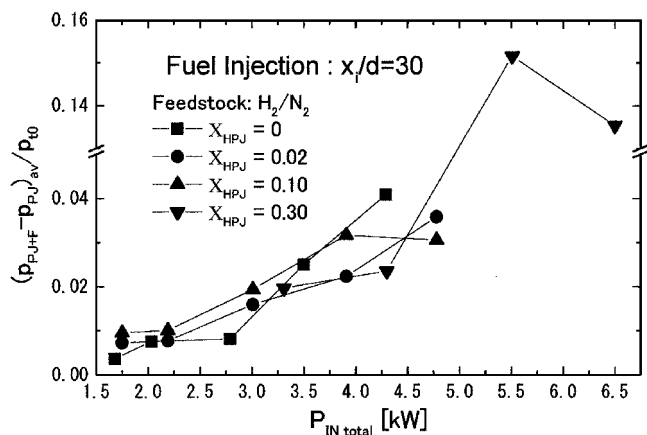
This result may not be surprising because the emission of the radical was rapidly decayed as the plasma jet went downstream. Takita et al.<sup>15</sup> measured the spatial distribution of the emission intensities of the  $N_2$  and  $O_2$  plasma jets in the same facility and found that the emission intensities became almost zero at  $x/d = 15$ , where fuel was not yet injected in the present experiment.

#### Total Input Power and Ignition

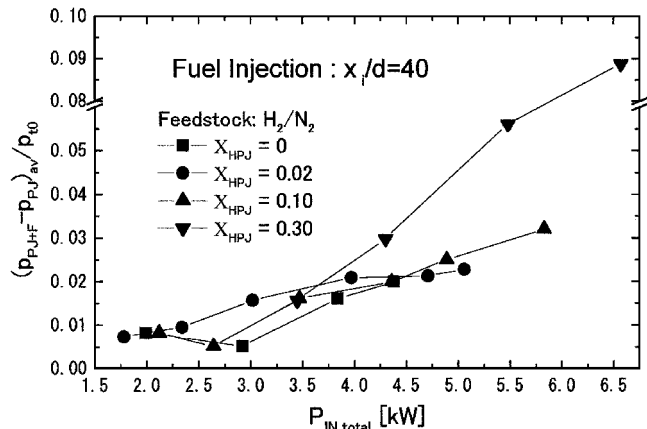
As discussed earlier, hydrogen in the feedstock burned in the airstream and released more heat in the flow. Therefore, the total power added to the airstream by the  $H_2/N_2$  plasma torch,  $P_{IN\ total}$ , should be represented by the sum of the electrical input power  $P_{IN}$  and the heat of combustion of the hydrogen fed through the torch,  $m_{HPJ}q_C$ . It would be more precisely estimated by multiplying  $P_{IN}$  by the thermal efficiency of the plasma torch and  $m_{HPJ}q_C$  by its combustion efficiency. However, as already discussed, the thermal efficiency of the torch was almost the same for all of the cases tested in the present experiment, and the combustion efficiency of the hydrogen in the plasma jet was estimated to be close to unity. Therefore, the terms of  $P_{IN\ total}$  used in this paper were not multiplied by the efficiencies.

Nondimensional mean pressure rise by fuel injection,  $(p_{PJ+F} - p_{PJ})_{av} / p_{t0}$ , is plotted to  $P_{IN\ total}$  in Fig. 13 for three values of  $x_i/d$ , namely, 30, 40, and 50. It is clearly seen that the pressure rise data are well correlated with the total input power. The nondimensional mean pressure rise remained less than 0.01 for  $P_{IN\ total} < 2.8$  kW, but it increased to 0.02 in a narrow region of  $2.8\text{ kW} < P_{IN\ total} < 3.0$  kW. Further increase of the total input power resulted in only a little increase of the pressure rise until the thermal choke modified the whole flowfield. The stepwise increase of the pressure rise, which indicated the ignition, occurred in the cases of  $x_i/d = 30$  and 50 at almost the same value of  $P_{IN\ total}$ .

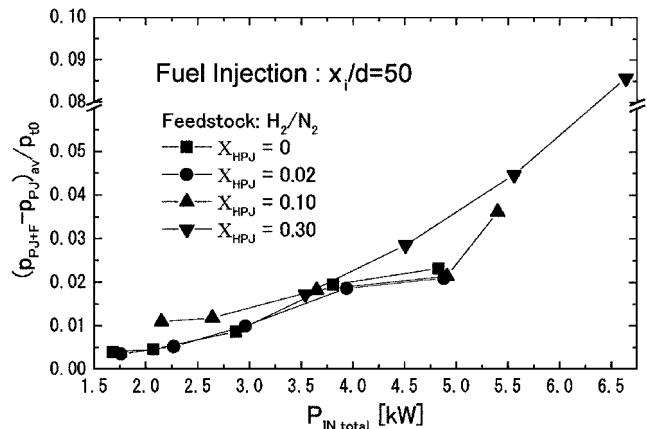
As shown in Fig. 13, the ignition limit of the plasma torch was well correlated by the total input power including both the electric input and the heat of combustion. This result indicates that the improvement in the ignition performance of the plasma torch by adding hydrogen to the feedstock is mainly due to the heat release



a)  $x_i/d = 30$



b)  $x_i/d = 40$



c)  $x_i/d = 50$

Fig. 13 Effect of total input power of plasma torch to mean pressure rise,  $M_0 = 1.8$ :  $\square$ ,  $X_{HPJ} = 0$ ;  $\circ$ ,  $X_{HPJ} = 0.02$ ;  $\triangle$ ,  $X_{HPJ} = 0.10$ ; and  $\nabla$ ,  $X_{HPJ} = 0.30$ .

by the combustion of hydrogen after the plasma jet is injected in the airstream. Along with the discussion about Figs. 10–12, the result also suggests that the main ignition mechanism of the plasma torch to the hydrogen injected downstream of the torch is addition of heat rather than radicals.

#### Conclusions

The effects of Mach number and pressure of airstream on the ignition performance of the  $H_2/N_2$  plasma torches were experimentally investigated. The effect of the hydrogen fraction of the feedstock was also studied. The main results are as follows.

Ignition of hydrogen fuel in higher Mach number airstreams required larger input power of the plasma torch igniter for the same stagnation conditions of the airstreams. The effect of the airstream

pressure on the ignition performance of the plasma torch was not clearly indicated because the boundary layer became easier to separate in the lower pressure. Addition of hydrogen to the nitrogen feedstock improved the ignition performance of the torch. The ignition limit of the  $H_2/N_2$  torch was well correlated with the sum of the heat of combustion of hydrogen in the feedstock and the electric energy input and suggests that the heat addition to the flow is the main mechanism of ignition by the plasma torch, when the hydrogen fuel was injected downstream of the torch.

### Acknowledgments

This study was partly supported by the Ministry of Education (Grant in Aid for Scientific Research 10555331 and 11750149). The authors are grateful to Masao Chiba of Tohoku University and Katsura Ohwaki and Masashi Matsumoto of Ishikawajima-Harima Heavy Industries for their assistance in fabricating the experimental apparatus.

### References

- <sup>1</sup>McClinton, C. R., "Autoignition of Hydrogen Injected Transverse to Supersonic Airstream," AIAA Paper 79-1239, June 1979.
- <sup>2</sup>Spadaccini, L. J., and Chinitz, W., "Supersonic Combustion of Propane," *AIAA Journal*, Vol. 6, No. 7, 1967, pp. 1391-1393.
- <sup>3</sup>Beach, H. L., Jr., Mackley, E. A., Rogers, R. C., and Chinitz, W., "Use of Silane in Scramjet Research," *17th JANNAF Combustion Meeting*, CPIA Publ. 329, Vol. 1, Chemical Propulsion Information Agency, Laurel, MD, 1980, pp. 639-659.
- <sup>4</sup>Kimura, I., Aoki, H., and Kato, M., "The Use of a Plasma Jet for Flame Stabilization and Promotion of Combustion in Supersonic Air Flows," *Combustion and Flame*, Vol. 42, 1981, pp. 297-305.
- <sup>5</sup>Northam, G. B., McClinton, C. R., Wagner, T. C., and O'Brien, W. F., "Development and Evaluation of a Plasma Jet Flameholder for Scramjets," AIAA Paper 84-1408, June 1984.
- <sup>6</sup>Masuya, G., Kudou, K., Murakami, A., Komuro, T., Tani, K., Kanda, T., Wakamatsu, Y., Chinzei, N., Sayama, M., Ohwaki, K., and Kimura, I., "Some Governing Parameters of Plasma Torch Igniter/Flame-holder in a Scramjet Combustor," *Journal of Propulsion and Power*, Vol. 9, No. 2, 1993, pp. 176-181.
- <sup>7</sup>Masuya, G., Chinzei, N., and Miki, Y., "Scramjet Engine Tests at Mach 4 and 6," *IUTAM Symposium on Combustion in Supersonic Flows*, Kluwer, Dordrecht, The Netherlands, 1997, pp. 147-162.
- <sup>8</sup>Kobayashi, K., Mitani, T., and Niioka, T., "Asymptotic Analysis of Plasma Jet Igniter," *Proceedings of the Twenty-First International Symposium on Space Technology and Science*, Agune, Tokyo, Japan, 1998, pp. 123-128.
- <sup>9</sup>Takita, K., Uemoto, T., Sato, T., Ju, Y., Masuya, G., and Ohwaki, K., "Ignition Characteristics of Plasma Torch for Hydrogen Jet in Airstream," *Journal of Propulsion and Power*, Vol. 16, No. 2, 2000, pp. 227-233.
- <sup>10</sup>Minato, R., and Niioka, T., "Three Dimensional Numerical Simulation of Combustion of Hydrogen Jet with Plasma Torch," *Proceedings of the Annual Meeting and the Ninth Symposium on Ram/Scramjets*, 1999, pp. 107-112 (in Japanese).
- <sup>11</sup>Kanda, T., Saito, T., Kudo, K., Komuro, T., Ono, F., and Matsui, A., "Mach 6 Testing of a Scramjet Engine Model," *Journal of Propulsion and Power*, Vol. 13, No. 4, 1997, pp. 543-551.
- <sup>12</sup>Masuya, G., Takita, K., Sato, T., and Ohwaki, K., "Ignition of Parallel and Low-Angle Hydrogen Jet by Plasma Torch," *Proceedings of the International Symposium on Air Breathing Engines*, Paper ISABE 99-7051, Sept. 1999.
- <sup>13</sup>Sato, Y., Sayama, M., Ohwaki, K., Masuya, G., Komuro, T., Kudou, K., Murakami, A., Wakamatsu, Y., Kanda, T., and Chinzei, N., "Effectiveness of Plasma Torches for Ignition and Flameholding in Scramjet," *Journal of Propulsion and Power*, Vol. 8, No. 4, 1992, pp. 883-889.
- <sup>14</sup>Sakuranaka, N., Mitani, T., Izumikawa, M., Sayama, M., and Ohwaki, K., "Thermal Efficiency of Plasma Torch Igniter," *Proceedings of the 33rd Space Science and Technology Conference*, 1989, pp. 56, 57 (in Japanese).
- <sup>15</sup>Takita, K., Takatori, F., and Masuya, G., "Effect of Plasma Torch Feedstock on Ignition Characteristics in Supersonic Flow," AIAA Paper 2000-3586, July 2000.
- <sup>16</sup>Sung, C. J., Li, J. G., Yu, G., and Law, C. K., "Chemical Kinetics and Self-Ignition in a Model Supersonic Hydrogen-Air Combustor," *AIAA Journal*, Vol. 37, No. 2, 1999, pp. 208-214.
- <sup>17</sup>Barbi, E., Mahan, J. R., O'Brien, W. F., and Wagner, T. C., "Operating Characteristics of a Hydrogen-Argon Plasma Torch for Supersonic Combustion Applications," *Journal of Propulsion and Power*, Vol. 5, No. 2, 1989, pp. 129-133.